RSC Advances

ROYAL SOCIETY OF CHEMISTRY

www.rsc.org/advances

Graphical Abstract

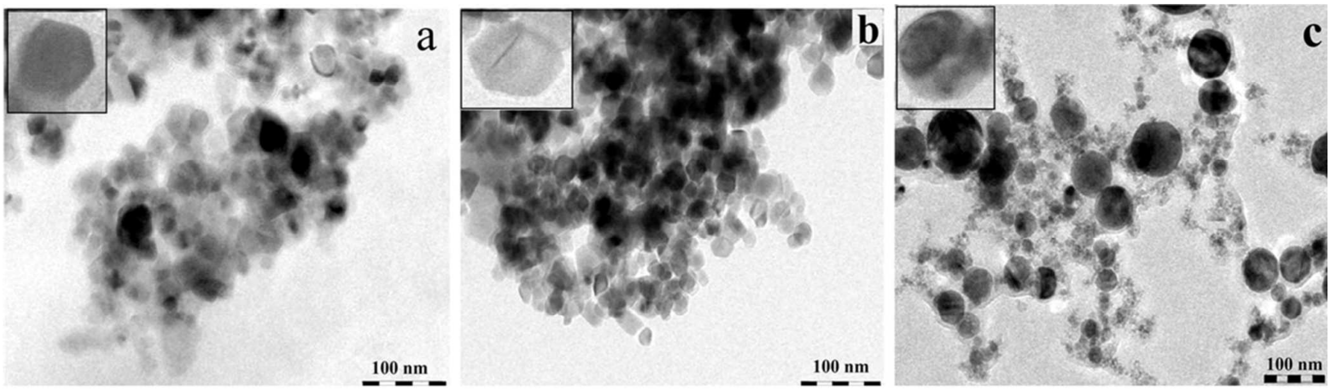

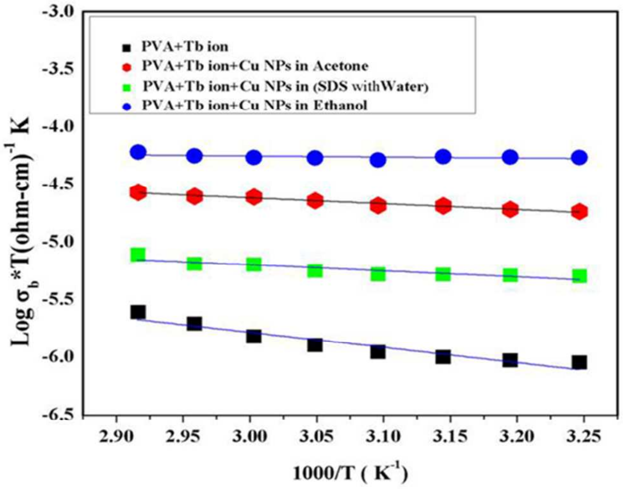

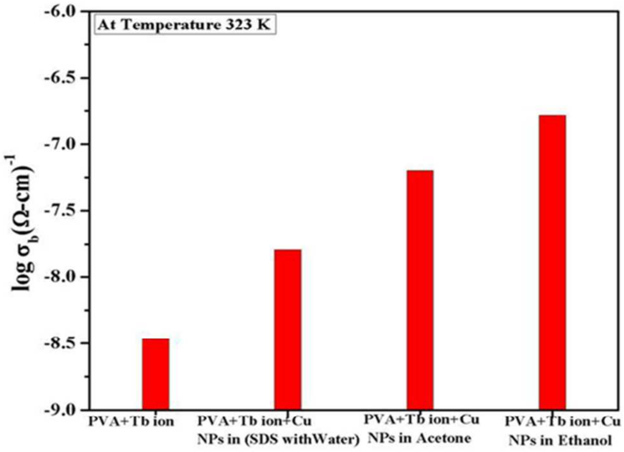

Anomalous Electrical Properties of Poly Vinyl Alcohol film with Tb^{3+} ion and Copper nanoparticles in different solvents

Brijesh Kumar[1], Gagandeep Kaur[1*], Prabhakar Singh[2], S. B. Rai[1]

[1]Laser and Spectroscopy Laboratory, Department of Physics,
Banaras Hindu University, Varanasi-221005 India
[2]Department of Physics, Indian Institute of Technology (BHU) Varanasi -221005 India

Abstract:

Laser ablation method has been used for fabrication of copper nanoparticles (NPs) in different solvents viz sodium lauryl sulphate, acetone and ethanol by applying 1064 nm radiation from Nd:YAG. The size and shape of colloidal Cu NPs have been investigated by transmission electron microscopy (TEM). The electrical conductivity of Tb^{3+} ion in polymer films with Cu NPs have been measured for frequency range between 20 Hz to 1 MHz and temperature range 308-343 K. It was found that the electrical conductivity of Tb^{3+} ion was maximum with bigger Cu NPs of size ranging from 20-40 nm in ethanol as compared to the Cu NPs formed of smaller dimensions in the other two solvents. It was concluded that ethanol as a solvent enhanced the electrical conductivity of Tb^{3+} ion in the polymer film. The activation energy as well as variation of loss tangent with temperature also explains the enhanced electrical conductivity.

PACS: **52.38.Mf; 82.35.Np; 81.07.Wx; 78.67.Bf**

Keywords: A. polymers; C. electron microscopy; D. electrical properties; D. electrical conductivity

Corresponding author: Dr. Gagandeep Kaur, Laser and Spectroscopy Laboratory, Department of Physics, Banaras Hindu University, Varanasi-221005, UP India Tel.: +91 – 542 - 2307308; Fax: +91 – 542 - 2368390.

E-mail address: gagandeep_bhu@yahoo.com

I. Introduction

Nanoparticle technology has wide applications in various fields in our day to day life [1]. Nanoparticles (NPs) exhibit unique electrical properties different from those of bulk metal due to quantum size effects. These properties can further be tuned by controlling the shape, size, interparticle spacing and dielectric environment. NPs of various elements viz Ag, Au, Pt., Si, C, Co etc. have been prepared to study their properties in nano regime and observe their influence on neighboring particles [2-6]. Copper (Cu) NPs are the focus of research now-a-days due to their interesting roll in, electrical, thermal and conducting properties [7, 8]. Fabrication process plays an important role on the properties of nanoparticles such as crystallite size, shape, particles size distribution etc. These factors strongly affect the electrical properties of the material. Various methods are used for the preparation of NPs [9]. Out of these, the pulsed laser ablation of metal target has attracted great attention due to its simplicity and purity [10-12]. It provides contaminant-free nanostructure particles in a desired solvent. This top down method facilitates one to produce nanoparticles in vacuum or in a desired atmosphere. Though the copper NPs produced by this method are highly unstable, they easily oxidize and precipitate immediately after the exposure in oxidizing medium. Synthesis of Cu nanoparticles by pulsed laser ablation of metal target in ambient gas and in non oxidizing liquid media plays a role in preventing oxidation of NPs [9, 13].

Polyvinyl alcohol is a semi-crystalline polymer. Its crystallinity depends on the synthesis procedure and physical aging [14, 15]. Its thin film is especially suitable as host matrix for mixing the colloidal solution of NPs prepared by laser ablation method [16, 17]. Doping of lanthanides into vinyl multiphase polymer system can induce changes in various properties of the complex. These complexes can be used as sensor, electrochromic displays and solid state lasers [18, 19].

The electrical behavior of doped copper nanoparticles in polyurethane has been studied by Valodkar et al. [20]. Frequency-dependent conductivity and its variation with temperature was the focus of their study. Bose et al. [21] prepared the nanoparticles of copper oxide by chemical route and measured both dc and ac electrical properties. To the best of our knowledge, little is reported in literature about the electrical properties of rare earth metals doped with copper nanoparticles in polymers. A rare earth metal exists in ionic state and it will be interesting to study the electrical properties of polymer films with Tb^{3+} ion containing Cu NPs.

In the present work, the focus is on the preparation of colloidal Cu-NPs in different solvents viz sodium lauryl sulphate (SDS) solution in distilled water, acetone and ethanol with the help of pulsed Nd-YAG laser. The ablation of a bulk copper target in different solvents was done by using 1064 nm laser line and to characterize them structurally. The different solvents were adopted as the different dielectric constant and dipole moment of the solvents may effect the stability, size, composition and electrical properties of the metal nanoparticles. Further, we have studied the electrical conductivity of the Tb^{3+} ion in PVA films with and without Cu NPs prepared in different solvents.

II. Experimental Details:

A. Materials:

A copper plate (99.99%), acetone, ethanol, sodium lauryl sulphate ($C_{12}H_{25}NaO_4S$, molecular weight 288.38), Terbium oxide (99.9%) and Polyvinyl Alcohol (mw14000) were used as starting materials. All the chemicals were purchased from Sigma Aldrich.

B. Methodology:

Preparation of copper nanoparticles:

Fig.1 shows the experimental setup for laser ablation to produce the nanoparticles. NPs of copper were prepared by laser ablation method in SDS solution, acetone and ethanol using 1064 nm laser radiation with pulse duration: 7 ns, repetition rate: 10 Hz and fluence 64 J /cm^2. With the help of converging lens of focal length 10 cm, the laser beam was focused on the copper target(thickness: 0.5 mm, size: 8×5 mm^2) containing 10 ml solution of different solvents. Diameter of focused laser beam on the copper target was 0.5 mm. The copper plate was ablated for 45 min with constant stirring every time.

Fig.1 (a, b, c) shows the basic principle for the formation of copper nanoparticles. When the laser beam is allowed to fall on the copper plate, a high temperature high pressure copper plasma is produced at the solid liquid interface (Fig.1a). An adiabatic expansion of the hot plasma allows quick cooling to produce copper clusters (Fig.1b). The copper clusters interact with the surrounding liquid solution to produce copper nanoparticles (Fig.1c). The copper plate was taken out from the solution and the prepared colloidal solution of Cu NPs was ultrasonicated upto four hours. The colloidal NPs were used for structural characterization and preparation of polymeric films with Tb^{3+} ion.

Preparation of polymeric film:

Polyvinyl alcohol (PVA), Terbium oxide (Tb_4O_7), hydrochloric acid (HCl) and colloidal Cu NPs prepared in different solvents by laser ablation method were used for the fabrication of four different polymeric films:

1. Film containing PVA +Tb^{3+} ion:

   $TbCl_3$ solution was prepared by heating 0.1g of Tb_4O_7 in 10 ml HCl at 150^{0}C separately 0.15g of transparent PVA solution in 5 ml distilled water was taken. Both the solutions were mixed and continuously stirred on magnetic stirrer at 800 rpm for 30 minutes. Then the resulting mixture were poured in petri dish and kept in oven under slow evaporation (at 50^0C). This resulted in PVA +Tb^{3+} ion polymer film.

2. Film with PVA +Tb^{3+} ion + Cu NPs in SDS:

   Same composition of $TbCl_3$ and PVA as used in preparation of sample 1 was taken. Further 10 ml colloidal solution of Cu NPs prepared in SDS were mixed and continuously stirred for 30 minutes. Then the mixtures were poured in petri dish and put in oven under slow evaporation (at 50^0C). Thus polymer films of PVA +Tb^{3+} ion +Cu NPs in SDS were obtained. A similar procedure was followed to prepare thin films corresponding to acetone (3) and ethanol (4).

C. Characterization of the samples:

Transmission electron micrographs were taken using a Technai $20G^2$ (Philips) Transmission Electron Microscope (TEM) equipped with the charge coupled device (CCD). Electrical properties of the thin films were measured with the help of Wayne Kerr precision impedance analyzer (6500-P) in the frequency range 20 Hz to 1 MHz. For this measurement, circular polymer film was cut and sandwiched between two circular silver discs and then placed in between two electrodes of measuring cell. The contact area of polymer films was 140.534 mm^2 and thickness was about 0.266 mm. Conductance G and the loss tangent D were measured with the help of impedance values. The impedance analyzer setting automatically controlled the temperature of the sample holder and monitored the data through the software. All the measurements were carried out in the temperature range 308-343K, well below the glass transition temperature of the polymeric film.

III. Results and discussion:

A. Structural Characterization using Transmission Electron Microscopy (TEM):

Cu-NPs prepared in different solvents were adhered onto a coated mesh, and the mesh was examined after being dried in vacuum. Fig. 2A shows the microstructure of the copper NPs in SDS solution (a), acetone (b) and ethanol (c) respectively and 2B shows the graph of size-distribution & particle size. The TEM images show the copper NPs in different solvents having different shapes (shown in the respective insets). In case of SDS and acetone, the Cu NPs are of hexagonal shape with average particle size ranging from 12 to 25 nm and 15 to 30 nm respectively. However the Cu NPs prepared in ethanol are spherical with particle size varying in between 20–40 nm. This is due to precursor (medium effects) that SDS may stabilize copper hydroxide and delay its conversion to copper oxide whereas the nanoparticles may be complexed with the carbonyl group at their surfaces when prepared in acetone [22]. Also, the dipole moment of acetone is higher to ethanol resulting in stronger bonds to the surface of NPs. This may also be due to that the dielectric constant of acetone is less than that of ethanol.

B. Electrical measurements

The frequency and the temperature-dependent conductance G was measured using the impedance analyzer. The conductivity was calculated by using relation

$$\boldsymbol{\sigma = \frac{GL}{A}\ (\Omega\mathrm{cm})^{-1}}\ , \qquad \textbf{(1)}$$

where σ is the real part of the conductivity, L is the thickness of the sample film and A is the area of the films. Fig. 3 shows the frequency dependence of the real part of conductivity of PVA with Tb^{3+} ion and PVA with Tb^{3+} ion and Cu-nanoparticles in different solvents at different temperatures. In Fig. 3 (a-d) the conductivity value in the low frequency range (below 100 Hz) is changing very slowly. Figures 3 a to c show an indication of almost frequency independent part below 100 Hz. Nevertheless, Fig. 3 d shows frequency independent part in low frequency regime (below 100 Hz). Due to limitation of the instrument, conductivity spectra could not be measured below 20 Hz. It appears that for the samples shown in fig. 3 a to c, the frequency independent part will clearly be visible below 20 Hz. In summary, the frequency independent part could not be observed in all the samples, however, a clear indication of frequency independent part in low frequency range is observed in all the samples. In any material, conduction occurs due to hopping motion of the charged particles. In the low frequency range when the time window is large, the ions and surroundings have enough time to rearrange themselves causing random hoping of the charge particles, giving rise to DC conduction. At the same time, at higher frequencies, the time window is small and therefore, the ions surroundings do not find enough time to rearrange themselves resulting into non-random correlated forward-backward hoping motions. This leads to an increase in conductivity value with increasing frequency, causing dispersion in the frequency spectra [23]. Thus, the real part of the conductivity spectra of these systems can be approximated as the sum of the dc and ac conductivities. Fig. 3 also shows that the conductivity increases on increasing the frequency in the dispersion regimes. The conductivity is maximum in the case of PVA film containing Tb^{3+} ions with Cu nanoparticles in ethanol.

The combined impedance of a sample expressed as $\boldsymbol{Z = Z' - i\,Z''}$ where $\boldsymbol{Z'}$ and $\boldsymbol{Z''}$ is the real and imaginary parts of impedance, respectively. These values are calculated from the relation

$$\mathbf{Z'} = \frac{\mathbf{D^2}}{\mathbf{G\,(1+D^2)}} \quad \textbf{and} \quad \mathbf{Z''} = \frac{\mathbf{Z\prime}}{\mathbf{D}} \quad , \qquad \textbf{(2)}$$

where D, is the loss tangent. Typical impedance plots for $\mathbf{Z}'$and $\mathbf{Z}''$ for all the polymeric samples at temperature 323K is shown in Fig.4. Fig.4 (a,b,c,d) shows the Cole Cole plots of PVA with Tb^{3+} ion (sample-1), PVA with Tb^{3+} ion and Cu NPs in SDS solution (sample-2), PVA with Tb^{3+} ion plus Cu NPs in acetone (sample-3) and PVA with Tb^{3+} ion and Cu NPs in ethanol (sample-4), respectively. The high frequency semicircle corresponds to bulk response of the polymer film. This arises due to migration of terbium ions in polymer matrix. Also it is controlled by the bulk resistance of the sample. The immobile polymer chain is polarized in the field of applied electric field. Thus migration of ion and bulk polarization is parallel in the semicircle region [24]. At low frequency region, spike characteristic behaves as blocking double layer capacitance [25]. This characteristic at low frequency is due to metal electrode interface and could be regarded as a capacitance. When the capacitance is ideal it should show vertical spike. However, in our case, the spikes in the Cole-Cole plot are inclined at an angle less than 90^0 which may be attributed to the roughness of the electrode interface [26, 27].

The bulk resistances R_b for polymer films have been calculated from the intercept of the semicircle in Fig.4 on the x- axis. The resistances of the polymer films at 323 K were found to be 2.7×10^6 Ω, 1.8×10^6 Ω, 4.5×10^5 Ω and 5.6×10^4 Ω for sample 1, 2, 3 and 4 respectively. Thus resistance is maximum for film with Tb^{3+} ion in PVA and minimum for film Tb^{3+} ion with Cu NPs in ethanol. The bulk conductivity of the samples were calculated using the relation

$$\boldsymbol{\sigma}_{\mathbf{b}} = \frac{\mathbf{L}}{\mathbf{R_b\,A}}\ (\mathbf{\Omega cm})^{-1} \qquad \textbf{(3)}$$

The bulk conductivity $\boldsymbol{\sigma}_{\mathbf{b}}$ for all four samples is plotted in Arrhenius representation in Fig.5 (a). It is clear from the figure that the systems follow linear behavior in the temperature region 308 K-343 K. The activation energy for conduction was calculated using Arrhenius relation

$$\boldsymbol{\sigma_b = \frac{\sigma_0}{T}\ exp\left(\frac{-E_a}{kT}\right)}\ \ (\mathbf{\Omega cm})^{-1}\ \ , \qquad \textbf{(4)}$$

where $\boldsymbol{\sigma_0}$ is the pre-exponential factor, $\mathbf{E_a}$ is the activation energy for conduction, k is the Boltzmann constant and T is the absolute temperature. The activation energy of polymer sample in temperature range 308 K-343 K is calculated by the linear fit of Fig. (5a) between log $\sigma_b * T$ [(ohm-cm)$^{-1}$ K] and 1000/T (K^{-1}) and the values thus obtained for the four samples are tabulated in table 1. A decreasing trend of activation energy is clearly evident from sample 1 to sample 4. This refers to increase in electrical conductivity, as we go from the polymer film with Tb^{3+} ion alone to that with PVA film with Tb^{3+} ion and Cu NPs in ethanol.

Variation of conductivity of polymeric samples in different solvents at 323 K is shown in Fig. 5 (b). The increase in conductivity from sample-1 to sample-4 can be understood as follows: In sample 1, when only Tb^{3+} ion are dispersed in PVA, the conduction is due to Tb^{3+} ion through the cross linked PVA chains. In sample 2 containing PVA with Tb^{3+} ion and Cu NPs in SDS solution, the conduction is due to Cu NPs moving through matrix of PVA+ Tb^{3+} ion cross linked chain. Individual Cu NPs and Tb^{3+} ion migrate among the vacant sites of the cross linked chain. The Cu-NPs increase in size and are agglomerated in acetone. Due to bigger size particles, small icelands are formed in sample 3, which contains PVA with Tb^{3+} ion and laser ablated Cu NPs in acetone, providing more conducting channels for the system and hence enhancing the conductivity. Considering sample 4 containing PVA with Tb^{3+} ion and Cu NPs in ethanol, further improvement in particle size provides more conducting channels for the free ion. This causes an increase in conductivity further in sample-4. The observed conductivity phenomenon, as explained above, for all the four samples is shown diagrammatically in Fig. 6. The TEM micrographs and the corresponding graph showing the particle size (Fig.2) also confirm the increase in particle size as we go from sample-2 to sample-4. This confirms our hypothesis for an increase in conductivity.

For confirmation of enhanced electrical conductivity further, we show variation of loss tangent with temperature at constant frequency in Fig.7 (a-c) for all four samples at 10 kHz (fig 7a), 100 kHz (fig 7b) and 1 MHz (fig 7c). These figures clearly depict that the loss tangent are low almost for all the samples but they show an increasing trend as we go from sample-1 to sample-4 (except first two points of sample-4 and last two points of sample 2 in fig. 7 a). The loss tangent is maximum at given frequency for sample-4 i.e. PVA with Tb^{3+} ion and Cu nanoparticles in ethanol. The loss tangent, D is actually defined as

$$\mathbf{D} = \frac{\epsilon''}{\epsilon'} = \frac{\sigma'}{\sigma''} \quad , \tag{5}$$

where $\boldsymbol{\epsilon'}$ and $\boldsymbol{\epsilon''}$ are the real and imaginary parts of the permittivity, respectively and $\boldsymbol{\sigma'}$ and $\boldsymbol{\sigma''}$are the real and imaginary parts, of the electrical conductivity, respectively. The above equation clearly reveals that higher the real part of conductivity larger is the loss tangent, which also explains the electrical behaviour of the four samples. This can be explained also in terms of Ohmic loss. Higher the conductivity larger will be the Ohmic loss and vice versa. The loss tangent basically represents the Ohmic loss (conduction loss) in any sample. Hence, the sample (sample-4) having maximum loss tangent will possess maximum conductivity.

IV. Conclusions:

Cu-NPs have been prepared in different solvents by laser ablation using 1064 nm wavelength from a pulsed Nd-YAG laser. TEM micrographs show hexagonal shaped Cu NPs in case of SDS solution and acetone but bigger spherical NPs in the case of ethanol. The electrical properties of Tb^{3+} ion in PVA polymer film with Cu NPs in different solvents have been studied. It is concluded that the electrical conductivity of Tb^{3+} ion in polymer films is maximum in the presence of bigger spherical Cu NPs prepared in ethanol. It is proposed that bigger size of nanoparticles in ethanol form more icelands in the polymer matrix causing an enhancement in electrical conductivity of the film. The activation energy and variation of loss tangent with temperature also confirm the enhanced electrical behavior of the samples.

Acknowledgments:

One of the authors Brijesh Kumar would like to acknowledge UGC for Meritorious fellowship in Science and G. Kaur would like to acknowledge DST for project grant.

References:

[1] M.C. Daniel, D. Astruc, Chem. Rev. 2004 **104** 293.

[2] W. Zhang, X. Qiao and J. Chen, Mater. Sci. Eng. B 2007 **142** 1.

[3] F. Mafune, J.Y. Kohno, Y. Takeda and T.Kondow, J. Phys. Chem. B 2003 **107** 4218.

[4] S. Yang, W. Cai, H. Zhang, X. Xu and H. Zeng, J. Phys. Chem. C 2009 **113**, 19091.

[5] A. Santagata, A.D. Bonis, A.D. Giacomo, M.D. Aglio, A. Laurita, G.S. Senesi, R. Gaudiuso, S. Orlando, R. Teghil and G.P. Parisi, J. Phys. Chem. C 2011 **115**, 5160.

[6] S. Husam, A. Salman and M.J. Abdullah, Mater. Sc. Eng. B 2013 **178**, 1048.

[7] X. Ren, D. Chen and F. Tang, J. Phys. Chem. B 2005 **109**, 15803.

[8] S.H. Wu and D.H. Chen, J. Colloid Interface Sci. 2004 **273**, 165.

[9] B. Kumar, G. Kaur, P. Singh and S.B. Rai, Appl. Phys. B 2013 **110**, 345.

[10] P.V. Kazakevich, V.V. Voronov, A.V. Simakin and G.A. Shafeev, Quantum Electronics 2004 **34**, 951.

[11] H.L. Aye, S. Choopun and T. Chairuangsri, J. Advanced Materials R. 2010 **93**, 83.

[12] V. Amendola and M. Meneghetti, Phys. Chem. Chem. Phys. 2009 **11**, 3805.

[13] F. Bouchait, C. Champeaux, H.S. Nagaraja, F. Rossignol, N. Lory, A. Catherinot, P.Blondy, and D Cros, Thin Solid Films 2004 **435,** 269**.**

[14] I. Dokme, S. Altındal, T. Tunc and I. Uslu, Microelectronics Reliability 2010 **50**, 39.

[15] D.D. Brunelli, T.D.Z. Atvars, I. Joekes and V.C. Barbosa, J. Appl. Polym. Sci. 1998 **69**, 645.

[16] G. Kaur, R.K.Verma, D.K. Rai and S.B. Rai, J. Lumin. 2012 **132**, 1683.

[17] T.N. Rostovshchikov, V.V. Smirnov, V.M. Kozhevin, D.A. Yavsin, M.A. Zabelin, I.N. Yassievich and S.A. Gurevich, Appl. Catal. A Gen. 2005 **296**, 70.

[18] D.K. Sardar, K.L. Nash, R.M. Yow and J.B. Gruber, J. Appl. Phys. 2007 **101**, 113115.

[19] E. Filippo, A. Serra and D. Manno, Sensors and Actuators B: Chemical 2009 **138**, 625.

[20] M. Valodkar, P.S. Rathore, P. Sharma, D. Kanchan, M. Patel and S. Thakorea, Polym. Int. 2012 **61**, 1745.

[21] A. Bose, S. Basu, S. Banerjee and D. Chakravorty, J. Appl. Phys. 2005 **98**, 074307.

[22] B. Kumar, G. Kaur, and S.B. Rai, Indian J Phys DOI 10.1007/s12648-014-0617-0.

[23] K. Funke, C. Cramer and D. Wilmer, in: Diffusion in Condensed Matter, P. Heitjans and J. Kärger eds., Sringer, Berlin, 2004

[24] C.G. Raptis, A. Patsidis and G.C. Psarras, eXPRESS Polymer Letters 2010 **4**, 234.

[25] U. Sasikala, P.N. Kumar, V.V.R.N. Rao and A.K. Sharma, Int. J. Eng. Sci. Adv. Tech. 2012 **2**, 722.

[26] A. Karthikeyan, P. Vinatier and A. Levasseur, Bull. Mater. Sci., 2000 **23**, 179.

[27] M. Hema, S. Selvasekerapandian, A. Sakunthala, D. Arunkumar, and H. Nithya, Physica B 2008 **403**, 2740.

Figure Captions:

Fig. 1: Experimental setup for laser ablation to produce the Cu nanoparticles by Nd:YAG laser

Fig. 2: (A) shows the microstructure of the copper NPs in SDS solution (a), acetone (b) and ethanol (c) respectively, inset to the figure shows the individual shape of nanoparticles in different solvents and 2(B) shows the graph of size-distribution & particle size.

Fig. 3: Variation of electrical conductivity versus frequency of polymeric films in the presence of Tb^{3+} ion and Tb^{3+} ion plus Cu NPs in different solvents at temperature range 308-343K.

Fig. 4: Cole –Cole plots of polymeric films in the presence of Tb^{3+} ion and Tb^{3+} ion with Cu NPs in different solvents at temperature 323 K (50^0C).

Fig. 5: (a) Arrhenius representation of bulk conductivity and (b) shows variation of bulk conductivity of polymeric films in the presence of Tb^{3+} ion and Tb^{3+} ion plus Cu NPs in different solvents.

Fig. 6: Pictorial representation for the conductivity phenomenon for Tb^{3+} ion in polymer film with copper NPs in different solvents.

Fig. 7: Variation of loss tangent with temperature at constant frequency of polymeric films.

Table Caption:

Table 1: Activation energy for polymeric films in the presence of Tb^{3+} ion and Cu NPs in different solvents.

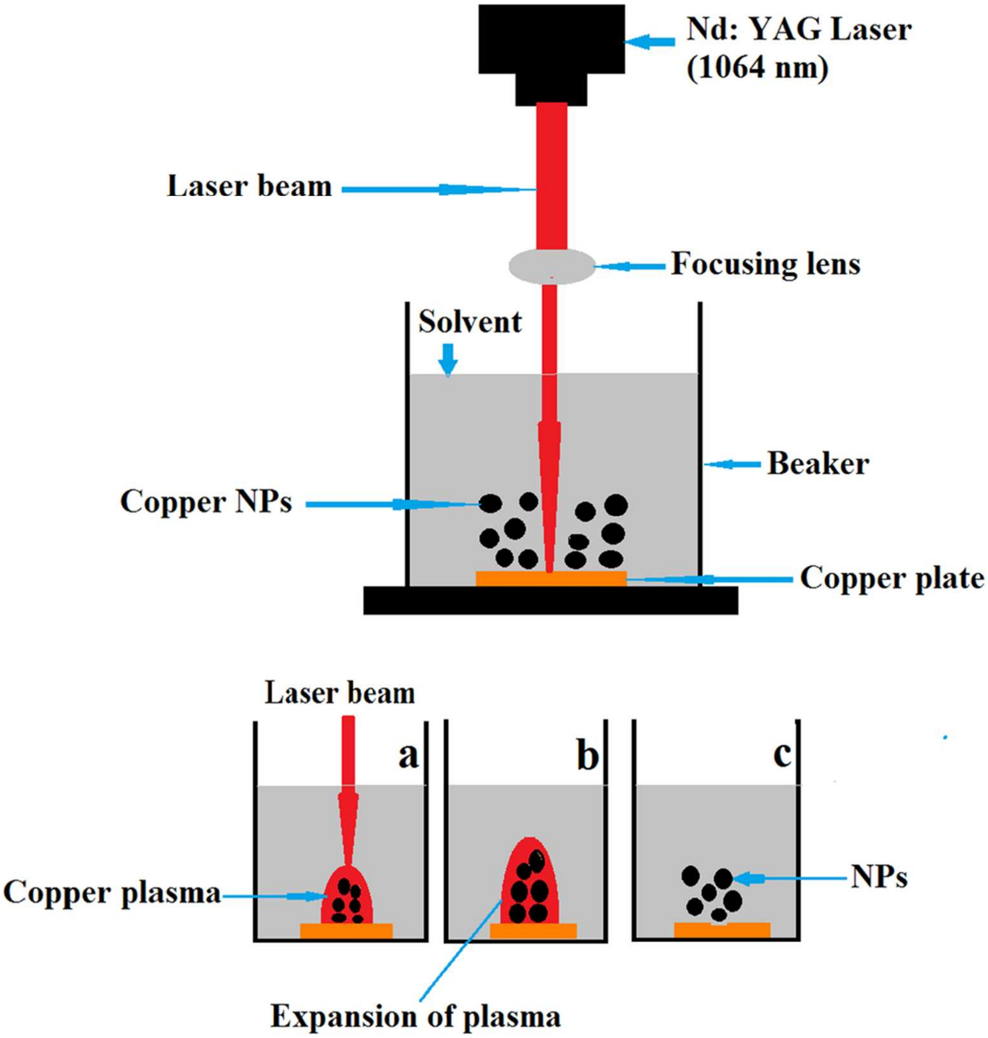

Experimental setup for laser ablation to produce the Cu nanoparticles by Nd:YAG laser
90x96mm (300 x 300 DPI)

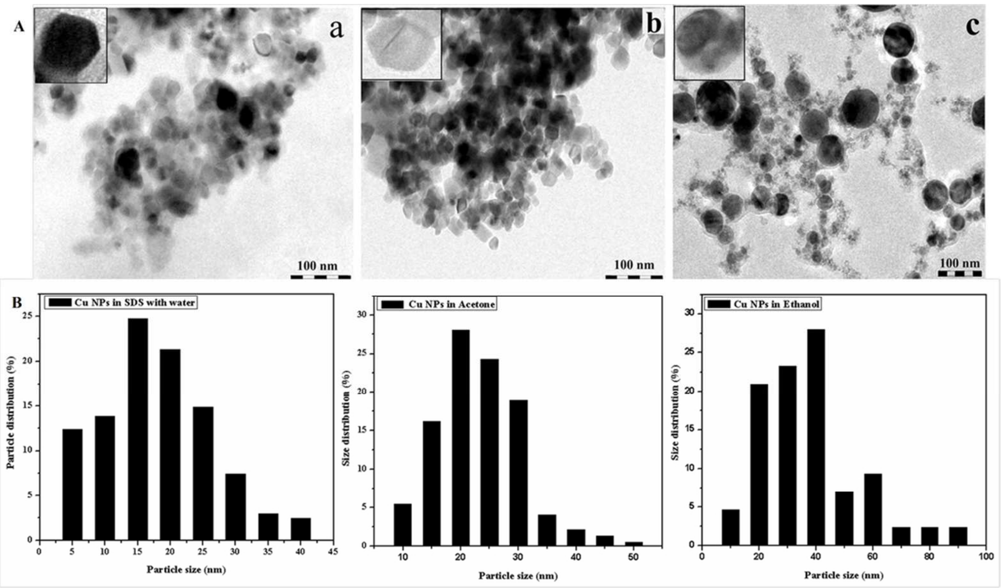

Fig. 2: (A) shows the microstructure of the copper NPs in SDS solution (a), acetone (b) and ethanol (c) respectively, inset to the figure shows the individual shape of nanoparticles in different solvents and 2(B) shows the graph of size-distribution & particle size.
99x58mm (300 x 300 DPI)

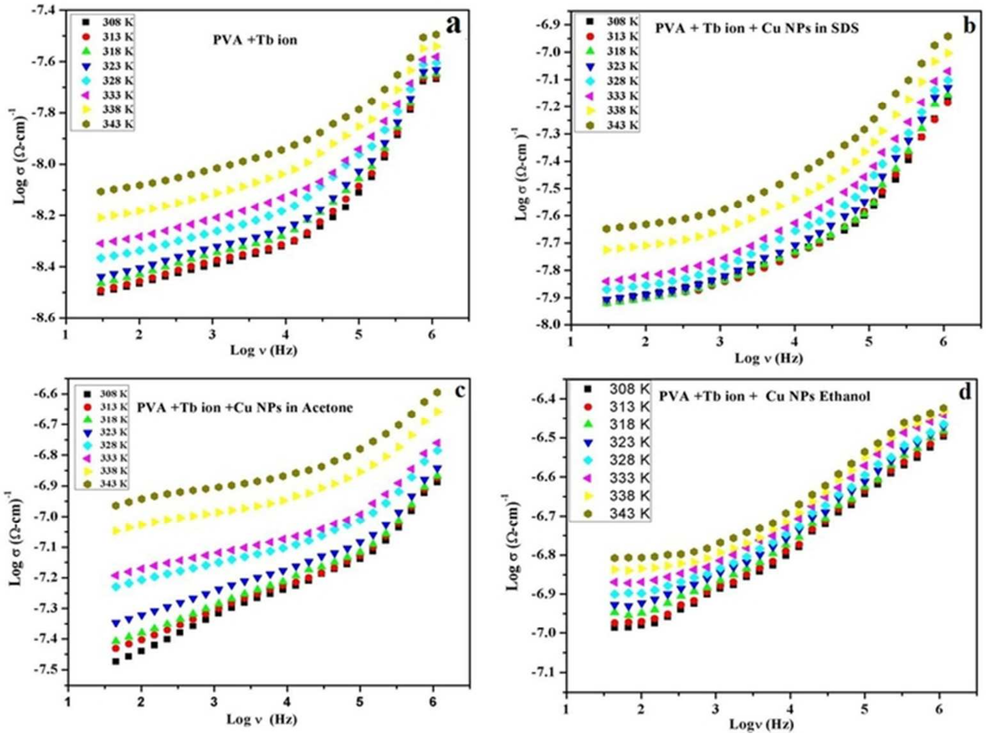

Variation of electrical conductivity versus frequency of polymeric films in the presence of Tb3+ ion and Tb3+ ion plus Cu NPs in different solvents at temperature range 308-343K.
62x45mm (300 x 300 DPI)

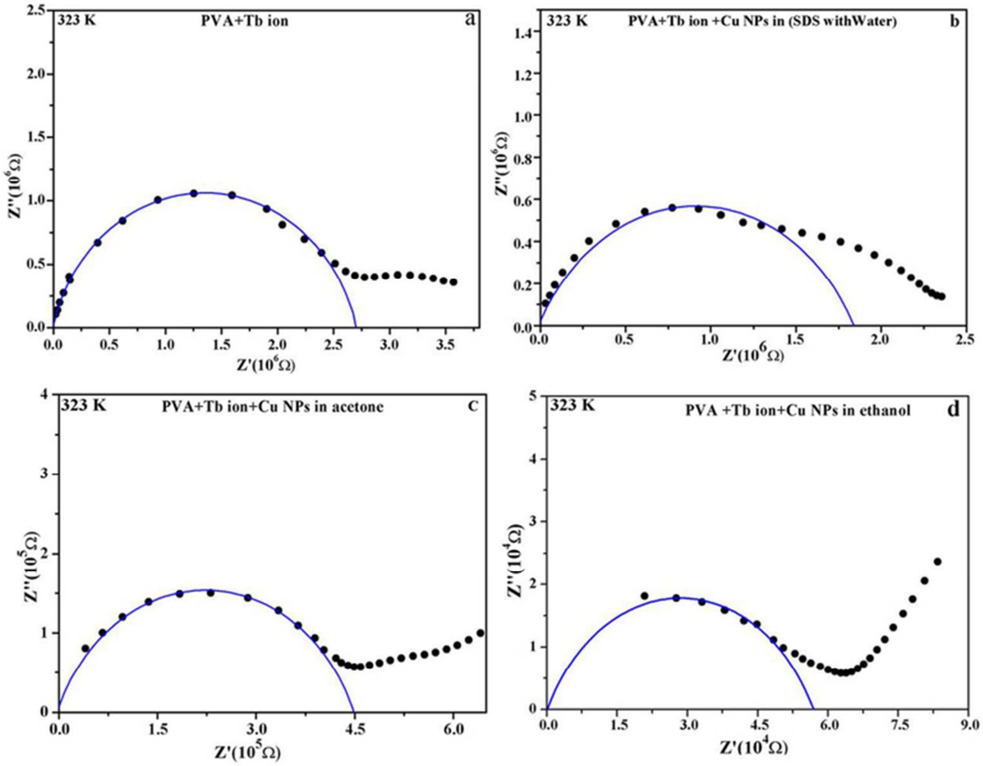

Cole –Cole plots of polymeric films in the presence of Tb3+ ion and Tb3+ ion with Cu NPs in different solvents at temperature 323 K (500C).
66x51mm (300 x 300 DPI)

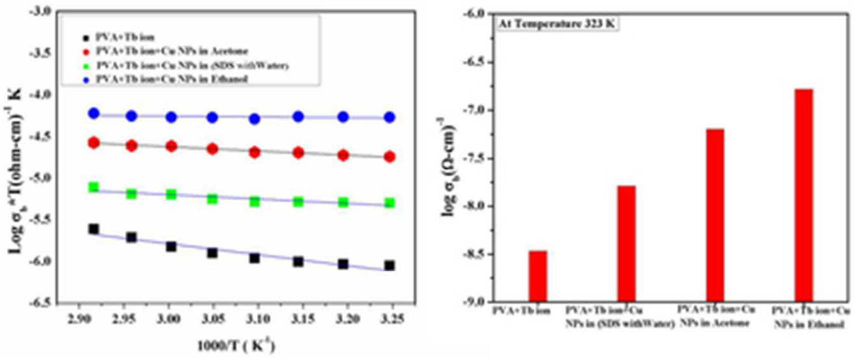

(a) Arrhenius representation of bulk conductivity and (b) shows variation of bulk conductivity of polymeric films in the presence of Tb3+ ion and Tb3+ ion plus Cu NPs in different solvents.
38x17mm (300 x 300 DPI)

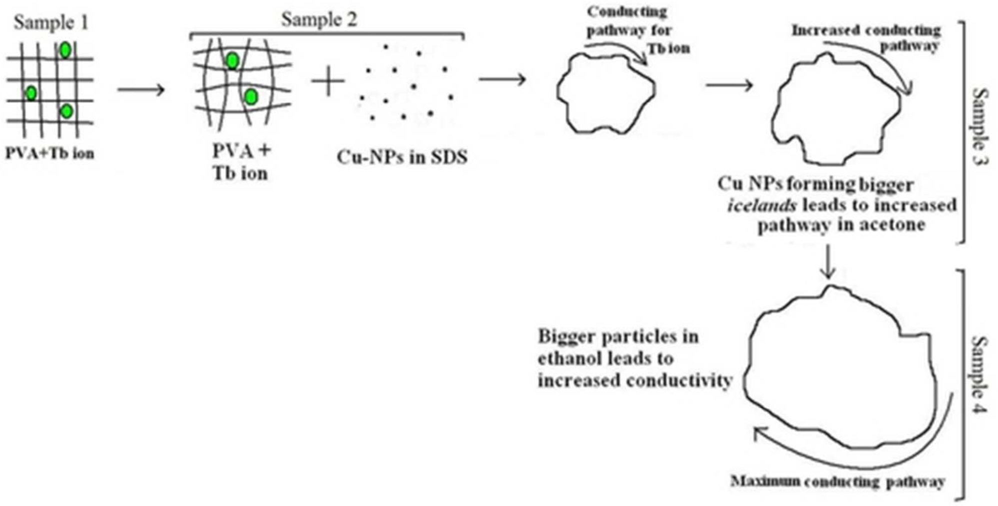

Pictorial representation for the conductivity phenomenon for Tb3+ ion in polymer film with copper NPs in different solvents.
43x22mm (300 x 300 DPI)

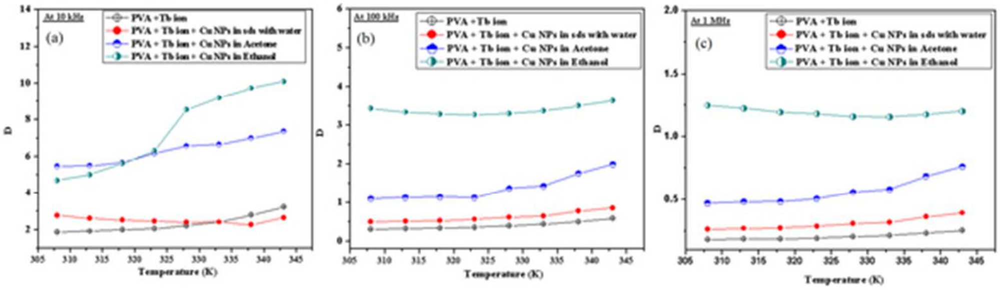

Variation of loss tangent with temperature at constant frequency of polymeric films.
49x14mm (300 x 300 DPI)

Table: Activation energy for polymeric films in the presence of Tb ion and Cu NPs in different solvents

Sample	**Activation energy**
	308K-343K
PVA+ Tb ion (Sample-1)	0.26 eV
PVA+ Tb ion+ Cu NPs in SDS with water (Sample-2)	0.11 eV
PVA+ Tb ion+ Cu NPs in Acetone (Sample-3)	0.10 eV
PVA+ Tb ion+ Cu NPs in Ethanol (Sample-4)	0.02 eV